Graphene surface plasmon bandgap based on two dimensional Si gratings

Mengjia Lu
Optical Information Science and Technology Department, Optoelectronic Engineering and Technology Research Center, Jiangnan University
Wuxi, China
1973780085@qq.com

Yueke Wang
Optical Information Science and Technology Department, Optoelectronic Engineering and Technology Research Center, Jiangnan University
Wuxi, China
ykwang@jiangnan.edu.cn

***Abstract*— A graphene/Si system, which is composed of a two-dimensional subwavelength silicon gratings and a graphene sheet, is designed to realize the complete band gap in infrared region for graphene surface plasmons (GSPs) theoretically. The complete band gap originates from the strong scatterings, which is caused by the periodical distribution of effective refractive index. The band structure has been calculated using the plane wave expansion method. Full wave numerical simulations are conducted by finite element method to verify the existence of band gap for in-plane GSPs. Thanks to the tunable permittivity of graphene by bias voltages or chemical doping, the band structure can be easily tuned, which provides a controllable platform to manipulate in-plane GSPs' propagation in infrared region.**

Keywords—Gratings; Plasmonics; Band gap; Graphene

I. INTRODUCTION

Surface plasmons (SPs), originating from the interaction between free electrons of metal and the electromagnetic waves, hold potential applications in highly integrated optical devices, because they can break the conventional diffraction limit [1, 2]. Graphene provides the platform of controlling SPs at infrared frequencies [3]. Compared with the counterpart in the visible and near-infrared frequencies, which propagates along the noble metal surface, graphene SPs (GSPs) show attractive properties, including higher confinement and relatively low propagating loss [4]. The propagation properties of GSPs can also be tuned by external gate voltages or chemical doping. A number of tunable plasmonic phenomena have also been studied such as nanofocusing [5] and sensors [6]. Photonic crystals (PCs) have attracted great attention due to their unique properties. When electromagnetic waves propagate through PCs, band structures are formed by Bragg scattering. The photonic band gaps (PBGs) can be obtained by spatially periodical dielectric constants. Light with a wavelength within the PBGs is not allowed to propagate through the PCs. Besides, a SPs analogy of photonic crystals is investigated both experimentally and theoretically, which provides a platform to manipulate the propagation of in-plane SPs [7]. But, the actively controllable band structures are barely investigated, and the research progress of GSPs offers a possible way.

In this paper, we propose a graphene structure, which is composed of a two-dimensional silicon gratings and a graphene layer. The complete band gap results from spatially periodical effective refractive index of the GSPs in infrared region. The band structure for in-plane GSPs is calculated by plane wave expansion (PWE) method; and finite element method (FEM) been used to full wave numerical simulations. Electromagnetic field distribution verifies the existence of band gap. Because the surface conductivity of graphene can be easily tuned by bias voltages or chemical doping, the band structure for in-plane GSPs can be actively controlled, which provides a platform to manipulate GSPs' propagation

II. STRUCTURE AND GSPS DISPERSION

The schematic of the silicon grating based system is illustrated in Fig.1. A Graphene sheet is on the top of the silicon gratings, which is composed of silicon cylinder arrays. The diameter D of the silicon cylinder is 18.45 nm. Silicon cylinders are arranged in a square mesh with a period of b = 41 nm. The refractive indexes of air and Si are set to be 1 and 3.44, respectively. Graphene/Si and graphene/Air interfaces can both support GSPs, which have different effective refractive indexes. When GSPs propagate along our proposed system, GSPs experience the periodic distribution of effective refractive index. So our proposed system is a GSPs analogy of photonic crystals. Strong scatterings of GSPs, which are caused by effective refractive index contrast, result in a complete band gap for GSPs at a specified frequency range.

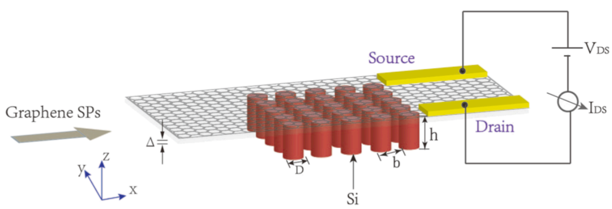

Fig. 1 Schematic illustration. The geometric parameters are b = 41 nm, D = 18.45 nm. The GSPs propagates along the graphene sheet. The thickness of graphene Δ = 1 nm.

Here, the surface conductivity of graphene σ_g is computed by the Kubo formula [8] as follows

$$\sigma_g = \frac{ie^2 k_B T}{\pi\hbar^2\left(\omega+i\tau^{-1}\right)} + \frac{ie^2}{4\hbar^2}\ln\left[\frac{2E_f-\left(\omega+i\tau^{-1}\right)\hbar}{2E_f+\left(\omega+i\tau^{-1}\right)\hbar}\right] + \frac{ie^2 k_B T}{\pi\hbar^2\left(\omega+i\tau^{-1}\right)\hbar}\ln\left[\exp\left(-\frac{E_f}{k_B T}\right)+1\right] \qquad (1)$$

Where k_B, T and $\hbar$ are the Boltzmann constant, the temperature, and the Plank's constant respectively. It is obvious that σ_g depends on momentum relaxation time τ, photon frequency ω and Fermi energy level $E_f=\hbar V_f(\pi n)^{1/2}$, where n is the charge carrier concentration, V_f= 106 m/s is the Fermi velocity. Considering the anisotropic nature of graphene [9], the in-plane permittivity $\varepsilon_{\|}$ of graphene is governed by:

$$\varepsilon = 1 + {i\sigma_g \eta_0}\big/{k_0\Delta} \qquad (2)$$

In the calculations, the graphene layer is treated as an anisotropic material with thickness Δ =1 nm, η_0 is the impedance of air, τ is chosen as 0.5 ps. The out-plane relative permittivity of graphene is $\varepsilon_\perp = 1$. As can be seen from Eqs. (1) and (2), the permittivity of graphene can be tuned by adjusting gate voltage or chemical doping, which therefore leads to a tuned Fermi energy value and enables the control of the propagation characteristics of the GSPs. In the mid-IR frequency range, such a conductivity form shows strong plasmonic response.

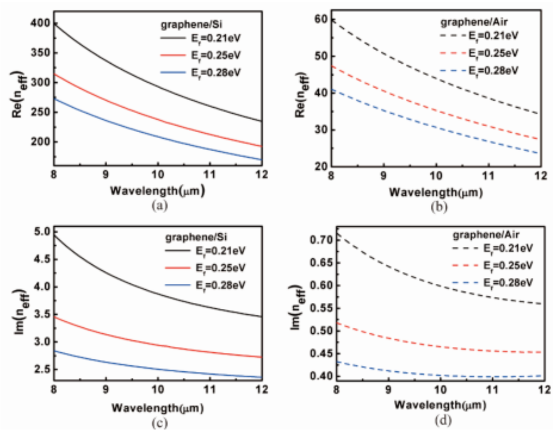

Fig. 2 Effective refractive index of the GSPs mode at graphene/silicon and graphene/air interfaces with wavelength under different Fermi energy levels. (a) Re(n_{eff}) and (c) Im(n_{eff}) for GSPs along the graphene/silicon interface; (b) Re(n_{eff}) and (d) Im(n_{eff}) for GSPs along the graphene/air interface

Firstly, we discuss the dispersion relations of the GSPs modes propagating along graphene/Si and graphene/Air interfaces. Fig.2 shows that real part (Re(n_{eff})) and imaginary part (Im(n_{eff})) of the effective refractive index for the GSPs mode, supported by graphene/Si and graphene/Air. Figs. 2(a) and (b) shows Re(n_{eff}) of GSPs mode supported by graphene/Si and graphene/Air interfaces under different Fermi energy levels, respectively. As the Fermi energy level increases, Re(n_{eff}) of GSPs mode decreases at a certain wavelength. And under a certain Fermi energy, Re(*neff*) of GSPs mode decreases while the wavelength increases. Re(*neff*) of GSPs mode on the graphene/Si interface is larger than that on the graphene/Air interface, and the high refractive index contrast benefits for the formation of a GSPs analogy of photonic crystals. So by forming a 2-dimensional Si gratings under the bottom of the graphene sheet, as shown in Fig. 1, one can manipulate the propagation of the GSPs by the band gap for the GSPs. It is seen from Figs. 2(c) and (d) that Im(n_{eff}) of GSPs mode at different Fermi energy level is also pictured.

III. GRAPHENE SURFACE PLASMON BANDGAP

There are three field components, Ex, Hy, and Ez, for the in-plane GSPs propagating along the graphene. Due to the boundary continuity, Ez component has been chosen to form eigenfunctions, which satisfies the Helmholtz equation.

$$\frac{1}{(n_{eff}(x,y))^2}\left(\frac{\partial^2}{\partial x^2}+\frac{\partial^2}{\partial y^2}\right)E_z(x,y) = \frac{\omega^2}{c^2}E_z(x,y) \qquad (3)$$

When GSPs propagates along the graphene/Si interface, n_{eff} is the effective refractive indexes of the GSPs mode supported by graphene/Si, and are obtained by Figs. 2(a) and (c). When GSPs propagates along graphene/air interface, n_{eff} is the effective refractive indexes of the GSPs mode supported by graphene/air, and are obtained by Figs. 2(b) and (d). By expanding $Ez(x, y)$ and $(n_{eff}(x, y))^2$ in reciprocal space, the eigenfunction of the GSPs photonic crystal can be as:

$$\sum_G (n_{eff})^2\left(\left|G-G'\right|\right)\left|k+G\right|\left|k-G'\right|E_z(G) = \frac{\omega^2}{c^2}E_z(G) \qquad (4)$$

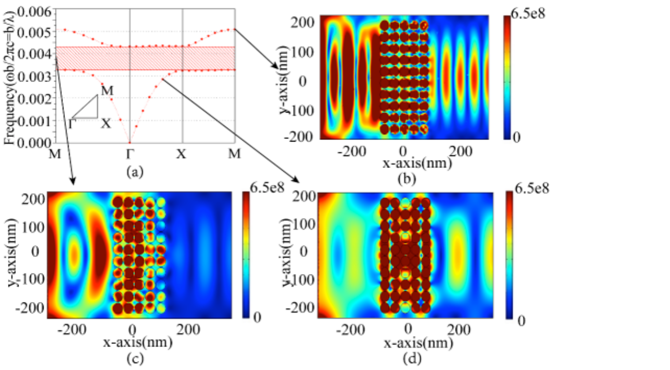

Fig. 3 (a) The band structure of in-plane GSPs, and the band gap is from 0.00326$\omega b/2\pi$c to 0.00429$\omega b/2\pi$c; H_y field distribution under different frequencies; (b) 0.00512$\omega b/2\pi$c locating at the second band, (c) 0.00371$\omega b/2\pi$c locating at the band gap and (d) 0.00293$\omega b/2\pi$c locating at the first band.

By solving Eq. (4) based on PWE method, we calculate the band structures at the Fermi energy E_f= 0.21eV, as shown in Fig.3 (a). The first band gap is from 0.00326$\omega b/2\pi$c to 0.00429$\omega b/2\pi$c, here c is the velocity of light in air. The band structure illustrates the in-plane GSPs, the frequency of which is within the band gap, can't propagate through the Si gratings, regardless of incidence angle. Based on the FEM method, we calculate the magnetic field distribution to validate the band structure by using COMSOL MULTIPHYSICS 5.0, as shown in Figs.3 (b)-(d). Fig.3 (b) shows the magnetic field distribution, for the GSPs propagating from left to the right when the normalized frequency of the incident light is 0.00512$\omega b/2\pi c$. Most of the incident GSPs can propagate through the silicon gratings region, which verifies the 0.00512$\omega b/2\pi c$ is in the second conduction band. Fig.3 (c) shows the magnetic field distribution, when the normalized frequency of the incident wave is chosen as 0.00371$\omega b/2\pi c$. GSPs can't pass through the silicon gratings, which verify the 0.00371$\omega b/2\pi c$ locates at the first forbidden gap. Fig.3 (d) shows the magnetic field distribution when the normalized frequency of the incident wave is chosen as 0.00293$\omega b/2\pi c$, which verifies the 0.00293$\omega b/2\pi c$ is in the first conduction band. Besides, the attenuation of GSPs in Figs.3 (b) and (d) originates from the absorption loss of graphene.

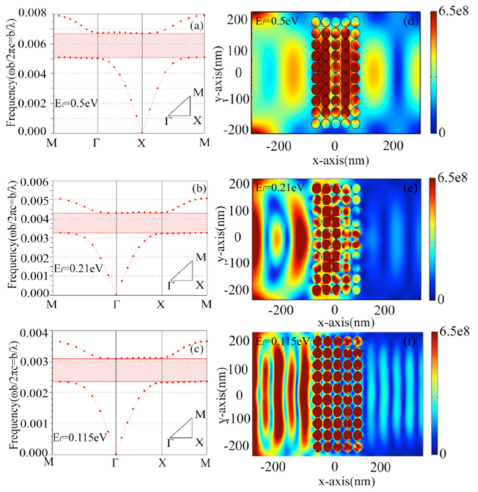

Fig.4 the band structures of GSPs when Fermi level of graphene is chosen as (a) 0.5eV, (b) 0.21eV and (c) 0.115eV. H_y field distribution when the incident wavelength is 11μm under Fermi level (d) 0.5eV, (e) 0.21eV and (f) 0.115eV.

Furthermore, the evolution of the plasmonic band structure with different Fermi level of graphene is also shown in Fig. 4. When E_f is chosen as 0.5eV, 0.21eV, and 0.115eV, the first band gap is from 0.00508$\omega b/2\pi c$ to 0.00669$\omega b/2\pi c$, from 0.00326$\omega b/2\pi c$ to 0.00429$\omega b/2\pi c$, and from 0.00233$\omega b/2\pi c$ to 0.00307$\omega b/2\pi c$, shown as Figs. 4(a), (b), and (c) respectively. The center wavelength of the band gap increases with E_f decreases. When we choose the work frequency (wavelength) as 0.00371$\omega b/2\pi c$ (11μm), the GSPs is in the first band when $E_f = 0.5$eV, in the band gap when $E_f = 0.21$eV and in the second band when $E_f = 0.115$eV. Figs. 4 (d) and (f) show that GSPs can propagate through the Si gratings, which demonstrates the work wavelength 11μm is in the first and second band, respectively. Fig. 4(e) shows GSPs hardly propagates through the Si gratings, which demonstrates the work wavelength 11μm is in the band gap. Thus, it is a smart way to tune the band structure of GSPs actively, by changing Fermi level of graphene. Our simulation results provide a method to design a tunable GSPs switch in infrared region. Our silicon/graphene system can be fabricated as follows: silicon gratings can be patterned by E-beam lithography, and the grephene can be grown by chemical vapor deposition (CVD) method.

IV. CONCLUSION

In conclusion, a GSPs analogy of photonic crystals is proposed in theory. Our model is composed of a gratings and a graphene sheet, and the band structure for GSPs can be calculated using the PWE method. A complete band gap of in-plane GSPs in infrared region can be formed, which is verified by the electromagnetic simulation using FEM method. Due to the tunability of graphene conductivity, the band structure of GSPs can be easily controlled. Thus, our simulation results provide a smart way to tune the GSPs' propagation along the graphene sheet actively. It is believed that tunable superfocusing, self-collimation, and negative refraction in infrared region, which are based on the dispersion relations of photonic crystal, will also be achieved.

V. ACKNOWLEDGMENT

This work was sponsored by the National Natural Science Foundation of China (11404143), Returned Overseas Fund of the Ministry of Education of China (1144130201150080). Postgraduate Research & Practice Innovation Program of Jiangsu Province (1145210232176730).

REFERENCES

[1] W. L. Barnes, A. Dereux, and T. W. Ebbesen, "Surface plasmon subwavelength optics," Nature, vol. 424, pp. 824–830, August 2003.

[2] D. K. Gramotnev, and S. I. Bozhevolnyi, "Plasmonics beyond the diffraction limit," Nat. Photonics, vol. 4, pp. 83-91, February 2010..

[3] M. Jablan, H. Buljan, and M. Soljacic, "Plasmonics in graphene at infrared frequencies," Phys. Rev. B vol. 80, pp. 245425, October 2009.

[4] W. Gao, J. Shu, C. Qiu, and Q. Xu, Q, "Excitation of Plasmonic Waves in Graphene by Guided-Mode Resonances," ACS Nano vol. 6, pp. 7806–7813, September 2012.

[5] S. Thongrattanasiri, F. H. L. Koppens, and F. J. Garc_ıa de Abajo, "Complete Optical Absorption in Periodically Patterned Graphene," Phys. Rev. Lett. vol. 108, pp. 0477401, January 2012.

[6] X. Yan, L. Yuan, Y. K. Wang, T. Sang, and G. F. Yang, "Transmittance characteristics and tunable sensor performances of plasmonic graphene ribbons," AIP Advances vol. 6, pp. 085301, August 2016.

[7] L. Feng, M. H. Lu, V. Lomakin, and Y. Fainman, "Plasmonic photonic crystal with a complete band gap for surface plasmon polariton waves," Appl. Phys. Lett. vol. 93, pp. 231105, July 2008.

[8] G. W. Hanson, "Quasi-transverse electromagnetic modes supported by a graphene parallel-plate waveguide," J. Appl. Phys. vol. 104, no. 8, pp. 084314, October 2008.

[9] M. Liu, X. Yin, E. Ulin-Avila, B. Geng, T. Zentgraf, L. Ju, F. Wang, and X. Zhang, "A graphene-based broadband optical modulator," Nature vol. 474, no. 7349, pp. 64-67, May 2011.